Acta Mech 226, 3823–3829 (2015)
DOI 10.1007/s00707-015-1406-3

ORIGINAL PAPER

Omid Nejadseyfi · Mahmoud Shamsborhan · Amin Azimi · Ali Shokuhfar

The roles of crystallographic orientation, high-angle grain boundary, and indenter diameter during nano-indentation

Received: 6 January 2015 / Revised: 14 June 2015 / Published online: 8 August 2015

Abstract Molecular dynamics simulation of nano-indentation of single-crystal and bicrystal FCC aluminum is performed. The role of crystallographic orientation during nano-indentation of single-crystal aluminum is assessed. Then, the influence of the presence of a grain boundary is analyzed by adding high-angle symmetric tilt boundaries of $\Sigma5<210>/(100)$ and $\Sigma5<310>/(100)$ parallel to the surface on which the indentation is performed. Furthermore, in both cases, the size of the indenter is changed to investigate how the surface curvature of the indenter affects the nano-indentation process. The results suggest that in each crystallographic orientation, the presence of a grain boundary increases the required force for indentation, while the distance of a grain boundary from the indentation surface could affect the increase in the required force. Simulations prove that the grain boundary acts as a source of generation and emission of dislocations and restricts the penetration of the indenter by limiting the slip band formation and plastic deformation. The dislocation emission from the grain boundary restricts the penetration of the indenter and limits the formation of the octahedral slip systems of type $\{111\}<110>$ and consequently increases the required force for indentation in bicrystals.

1 Introduction

Investigations on the governing mechanisms during indentation of different materials open a new horizon for cutting-edge applications and technologies, specifically those related to the development of nanostructured materials and thin films. Although the atomistic investigations in the nanoscale are challenging approaches to predict the behavior in physical conditions and environments, it is confirmed that atomistic simulations resemble the characteristics of the macroscopic scale reasonably [1–3].

Nano-indentation is widely used to investigate the mechanical properties of thin films. The penetration depth and required force for indentation on the nanoscale depend on the presence of several microstructural defects. Despite widespread use of crystalline materials in pioneering applications, most of the recent atomistic simulations have concentrated on the investigation of the behavior of the crack in single crystals [4–6]. Understanding the effects of grain boundaries on the material behavior and microstructural changes during

O. Nejadseyfi (✉) · A. Shokuhfar
Advanced Materials and Nanotechnology Research Lab, Department of Mechanical Engineering, K.N. Toosi University of Technology, Tehran 193951999, Iran
E-mail: o.nejadseyfi@sina.kntu.ac.ir; o.nejadseyfi@gmail.com
Tel.: +98 218406 3224; +98 914 454 0695
Fax: +98 21 8867 7274

M. Shamsborhan
Department of Engineering, Mahabad Branch, Islamic Azad University, Mahabad, Iran

A. Azimi
Young Researchers and Elite Club, South Tehran Branch, Islamic Azad University, Tehran, Iran

nano-indentation can provide significant information about this process. For coarse-grained materials, it is possible to assume that the indenter is far from grain boundaries and to neglect the effects of grain boundaries. However, for nanostructured materials and coatings, this assumption is not valid.

The behavior of grain boundaries has been studied in most recent works to reveal their influence on mechanical properties. Among these works, Nair et al. [7] simulated the nano-indentation process on Ni thin films using low-angle grain boundaries (LAGBs), which were generated perpendicular to the indentation surface. They showed that LAGBs act as dislocation sources and dislocations are emitted from those boundaries. Kim et al. [8] simulated the nano-indentation process on a nickel bicrystal with a $\Sigma 5 <210>$ grain boundary. Their results demonstrated that the dislocation nucleation is in the shape of prismatic loops. The study of nano-indentation of bilayers was also performed in recent studies [1,9,10].

Material behavior during nano-indentation is strongly dependent on several parameters, e.g., loading conditions, crystallographic orientation, temperature, indenter shape, indenter size, imperfections, and defects. The careful assessment of microstructural evolution is beneficial to reveal the contribution of the different parameters in nano-indentation. MD methods effectively develop the relation between the mechanical properties and microstructure of the material and provide a good understanding of the deformation mechanisms on the atomic scale. In addition, in simulations of nano-indentation, the influence of grain boundaries, particularly those located parallel to the indentation surface, gained less attention in the literature. Therefore, in this paper, MD simulations are employed to investigate the evolution of the microstructure during nano-indentation. For this purpose, the influences of indenter diameter, crystal orientation, and the presence of a symmetric tilt grain boundary are investigated during loading, and the results are discussed.

2 Atomistic simulation

The open source MD code Large-scale Atomic/Molecular Massively Parallel Simulator (LAMMPS) [11] and the Open Visualization Tool (OVITO) [12] were employed for atomistic simulations and visualization. Three-dimensional MD simulation of nano-indentation was performed using the embedded-atom-method (EAM) inter-atomic potential of aluminum [13]. This potential was reliably used to describe the bonding in metallic systems and to correlate the strength of individual bonds to the modeled system [14–17]. The total energy for an atom was calculated as follows:

$$E_i = F_\alpha \left(\sum_{j \neq i} \rho_\beta \left(r_{ij} \right) \right) + \frac{1}{2} \sum_{j \neq i}^{N} \emptyset_{\alpha\beta} \left(r_{ij} \right). \tag{1}$$

The first part of this equation was an embedding function, and the second part was the short-range electrostatic pairwise potential. The first term was a function of the distance between two atoms (r_{ij}) within a cutoff distance (F_α), and the second term was a function of the distance (r_{ij}) and the pair potential between two atoms $\emptyset_{\alpha\beta}$.

During the nano-indentation process, the temperature of the system was kept constant (300 K). As shown in Fig. 1, the simulation box was approximately 16 nm × 8 nm × 16 nm in the x, y, and z directions, respectively. Subsequently, indentation was performed in y direction considering periodic boundaries in x and z directions. The indentation force for the penetration of the indenter in the samples was recorded. The atomic stress field was also used in this work, defined as:

$$\sigma_{\alpha\beta}(i) = -\frac{1}{2\Omega_i} \sum_{j \neq 0}^{N} r_\alpha(i, j) F_\beta(i, j). \tag{2}$$

In this equation, N is the number of atoms surrounding atom i within the EAM potential cutoff distance, $r_\alpha(i, j)$ denotes the relative position of two atoms, $F_\beta(i, j)$ represents the interaction force exerted by atom j on atom i, and W_i is the volume of atom i. The average atomic stress tensor for each atom was calculated by taking an average over the volume around atom i within the potential cutoff distance as follows:

$$\bar{\sigma}_{\alpha\beta}(i) = \frac{1}{N} \sum_{j=1}^{N} \sigma_{\alpha\beta}(j). \tag{3}$$

In the first part of the paper, the influence of crystallographic orientation was assessed during loading. Three different crystal orientations were considered. In the first case, the x axis, y axis, and z axis in the simulation

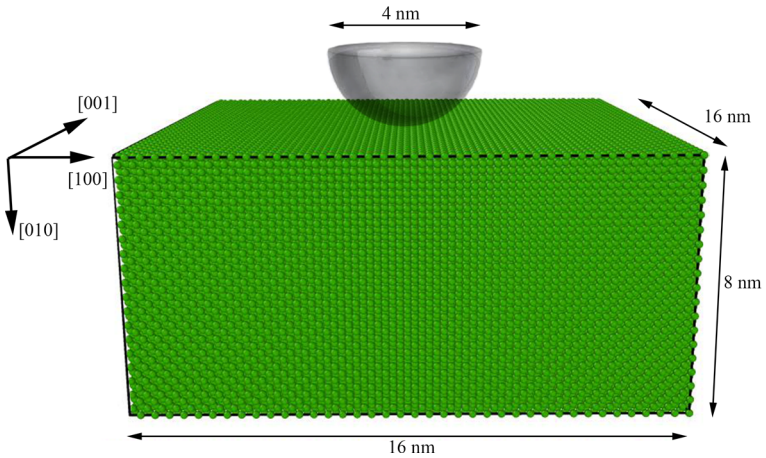

Fig. 1 Schematic illustration of nano-indentation

box were at [100], [010], and [001] lattice directions, respectively. In the second case, the x axis, y axis, and z axis in the simulation box were at [210], $[\bar{1}20]$, and [001] lattice directions, respectively. In the last case, x, y, and z axes in the simulation box were at [310], $[\bar{1}30]$, and [001] lattice directions, respectively. In all cases, the indentation was performed in y direction. In the second part, the influence of the presence of $\Sigma5<210>/(100)$ and $\Sigma5<310>/(100)$ high-angle grain boundaries (HAGBs) was assessed. In order to examine the nano-indentation process in bicrystals, high-angle symmetric tilt grain boundaries of $\Sigma5<210>/(100)$ and $\Sigma5<310>/(100)$ were generated in the distances of $D = 2$ nm, $D = 4$ nm, and $D = 6$ nm below the indentation surface. Each grain boundary plane was oriented parallel to the indentation surface. Finally, two different indenter diameters of $d = 4$ nm and $d = 8$ nm were implemented to study the influence of indenter size while the indentation depth was constant ($\sim$2 nm).

3 Results and discussion

Figure 2 illustrates the required force during indentation for different crystal orientations when the indenter diameter is $d = 4$ nm. To validate the results, the alteration in the required load observed in different crystallographic orientations of single crystals is compared with previous studies. The results show good coincidence with the simulations of Ju et al. [18] who investigated the nano-indentation process on single-crystal nickel with three different crystallographic orientations. As illustrated in Fig. 2, the required force for the case X[100] is higher than that in the other cases. The required force is reduced when the single crystal is rotated by 18° and 27°. Nevertheless, in each of these cases, the required force for indentation is increased by adding a HAGB. In order to investigate the reasons for this phenomenon, Fig. 3 illustrates the cross section of the sample during indentation. Common neighbor analysis (CNA) is used to detect the evolution of crystal defects. This method is a helpful measure of the local crystal structure around an atom, in which a characteristic signature is computed from the topology of bonds that connect the surrounding neighbor atoms. More details about the detection of crystal defects and specific dislocations are presented elsewhere [19].

The plastic deformation beneath the indenter and the high stress level of atoms in this region are main contributors to the slip initialization and generation of slip bands. Therefore, slip band generation is directly correlated with the high shear stress in this region. The amount of plastic deformation beneath the indenter prescribes the slip band generation. In Fig. 3a, b, slip occurs along a close-packed plane and the slip system is $\{111\}<110>$. However, the presence of a grain boundary delays further slip as depicted in Fig. 3b, and consequently, the required force for indentation is increased as shown in the diagram in Fig. 2. Nair et al. [7] observed that for relatively thicker films, the dislocations were emitted from the grain boundaries and in the single crystals the dislocations were emitted from underneath the indenter, which is consistent with the observations in this work.

The indentation force is actually dependent on the size of the indenter. Comparing Figs. 2 and 4 implies that when the diameter of the indenter is changed from 4 to 8 nm, the required force for indentation is increased by around 120 %. The increase in surface area and surface curvature are the main contributors to increasing the

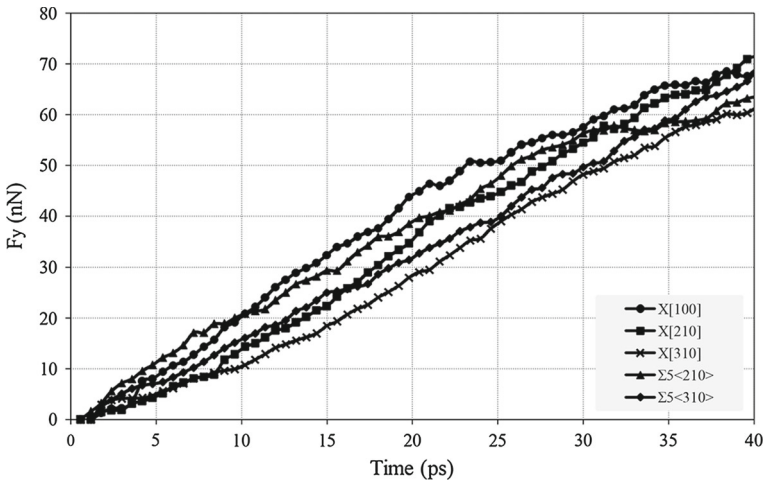

Fig. 2 Required force for indentation for an indenter using $d = 4$ nm

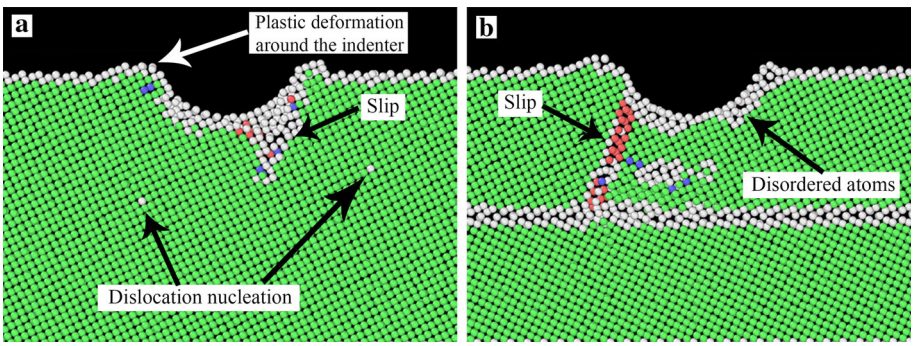

Fig. 3 Plastic deformation, dislocation nucleation, and slip band formation during nano-indentation in the absence and presence of a grain boundary for a specific crystallographic orientation

required force. These results are in agreement with the results of Muhammad et al. [20] who investigated the effects of the indenter diameter on the nano-indentation of single-crystal Ni. They showed that the maximum indentation force is higher for an indenter with a larger diameter than that for an indenter with smaller diameter. In addition to that, Fig. 4 indicates that the required force for indentation becomes higher in the presence of a grain boundary in each crystallographic orientation. As the grain boundary is a source of generation and emission of dislocations, it could restrict the penetration of the indenter by limiting the slip band formation. In this case, a higher force is required to be exerted on the sample to achieve the same penetration depth.

Figure 5 illustrates the dislocation emission and slip band formation when the diameter of the indenter is increased. As shown in this figure, while the sample is indented using an indenter with a larger diameter, the number of dislocations emanating from the grain boundary increases. The dislocation emission from the grain boundary restricts the penetration of the indenter and limits the formation of the octahedral slip systems of type {111}<110>, and consequently, the required force for indentation is increased in bicrystals. However, in single crystals with different crystallographic directions, the slip band formation requires a lower amount of normal force. Furthermore, as the misorientation angle between two grains is increased, the required force for indentation notably increases. This observation can also be explained considering the dislocation emission from the grain boundary, which seems to happen easily by increasing the misorientation angle between two grains.

It is confirmed that in the early stages of dislocation nucleation, dislocation slips along the slip plane and, when the dislocation expansion is hindered, the dislocation locks are formed and the dislocations finally end at the side surface composing "V"-shaped dislocation [21]. The presence of a grain boundary may enhance the hindering of dislocation glide while increasing the required force for indentation. Kim et al. [22] investigated the interaction between lattice dislocations and the $\Sigma 5$<210> symmetric tilt grain boundary, in which the grain boundary plane was normal to the indentation surface. They showed that the dislocation loops merged into

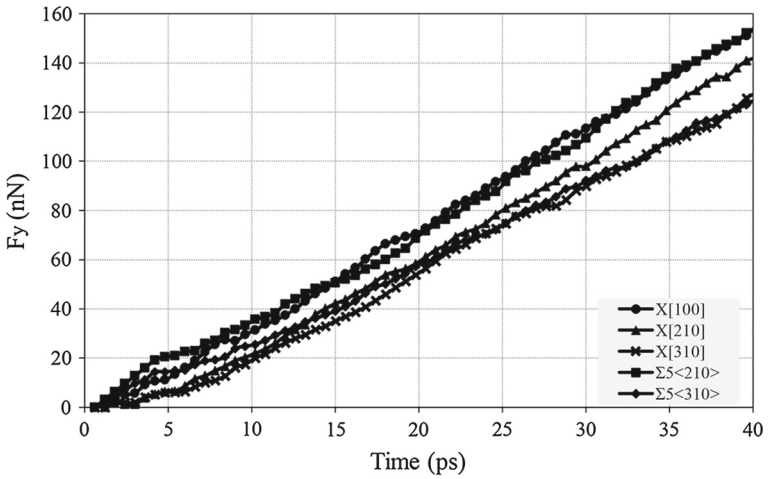

Fig. 4 Indentation force for an indenter with $d = 8\,\text{nm}$ and $D = 4\,\text{nm}$

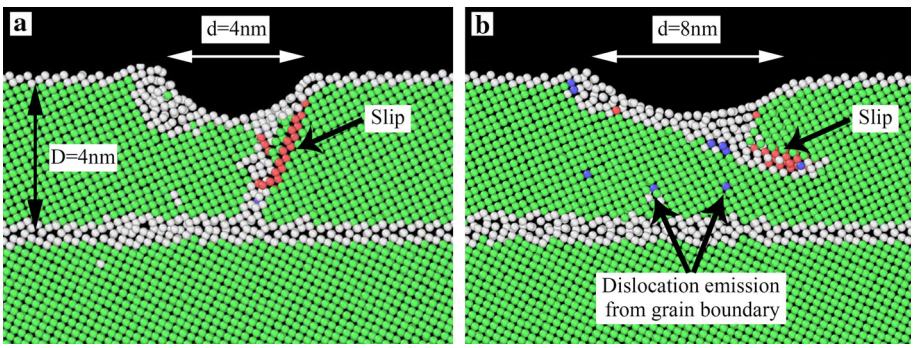

Fig. 5 Plastic deformation, dislocation nucleation, and slip band formation during nano-indentation with different indenters while $D = 4\,\text{nm}$

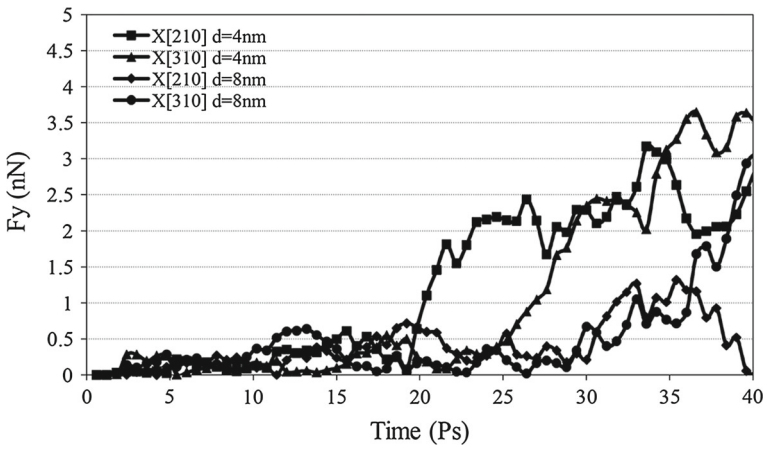

Fig. 6 Required lateral force (F_x) for nano-indentation

the grain boundary without emitting new dislocations to the neighboring grain. They correlated the migration of the Σ5<210> grain boundary after interaction with lattice dislocations to the nature of symmetric tilt boundaries that keep up a periodic set of grain boundary dislocations at the interface.

Although shear-coupled grain boundary migration is thermally activated, it can take place at relatively low temperatures. Shear-driven grain boundary migration at low temperatures is usually a consequence of the applied shear stress in which the grain boundary movement is perpendicular to the plane that contains

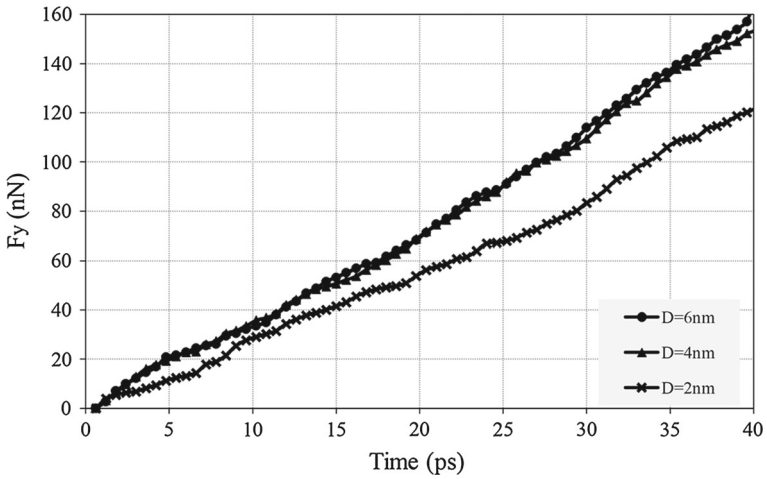

Fig. 7 Indentation force for indentation using $d = 8$ nm by changing the distance between grain boundary and surface

the boundary. A theoretical model was proposed by Li et al. [23] to illustrate the influence of shear-coupled migration of grain boundaries on the crack growth in nanocrystalline materials. They correlated the initiation of shear-coupled migration with the stress concentration in the vicinity of the crack tip in the mode I crack. They found that the coupled shear played a key role in enhancing the fracture toughness of nanocrystalline materials, and the shear-coupled migration that occurred served effective toughening mechanism in nanocrystalline materials. Although the grain boundary migration is usually observed at high temperatures, in the case where an external stress is applied to a nanocrystalline solid at room temperature, a normal grain boundary migration occurs. In addition, this normal grain boundary migration is usually accompanied by a tangential translation of grains parallel to the grain boundary plane for both LAGBs and HAGBs. Consequently, the translation would produce shear deformation of the lattice traversed by grain boundary, as proved by many molecular dynamics and quasi-continuum studies for bicrystals [24,25]. The fact that Kim et al. [22] observed boundary migration during nano-indentation seems to have originated from the orientation of the grain boundary plane with respect to the indentation direction. However, in this work, such a phenomenon was not observed, because the orientation of the grain boundary plane is normal to the indentation direction. In addition, other parameters such as penetration depth, indenter speed may affect the material behavior.

To investigate the differences between using different indenters, Fig. 6 depicts the required lateral force (F_x) during nano-indentation in bicrystals for which the value of D is 4 nm. This figure shows that, as the surface curvature of the indenter is increased, the lateral indentation force is reduced significantly. In addition to that, as the misorientation angle between two grains is increased, the required lateral force is also increased. Moreover, the effect of the distance between grain boundary and indentation surface is illustrated in Fig. 7. The required force for indentation drops more than 20 %, when the grain boundary is near to the indentation surface. In this case, the indenter penetrates through the grain boundary, leading to slip band formation and dislocation emission in the adjacent grain. Nevertheless, when the grain boundary is outside of the indenter penetration region, the required force does not show a significant variation.

It should be noted that although this work provides for the role of the presence of the grain boundary during nano-indentation, the interaction between grain boundaries is very important to assess the behavior of the materials under indentation. Therefore, more cases that are complicated should be addressed in future studies to clearly understand the material behavior during indentation.

4 Summary and conclusions

In this work, molecular dynamics simulation of nano-indentation process was performed on pure aluminum. The influence of indenter diameter was investigated in the presence and absence of a symmetric tilt grain boundary. In the single crystal, the required force for the case X[100] was higher than that in other cases, and when the single crystal was oriented in X[210] and X[310] directions, the required force was reduced. However, by adding high-angle symmetric tilt grain boundaries of $\Sigma5<210>/(100)$ and $\Sigma5<310>/(100)$ to the X[210] and X[310] cases, respectively, the required force for indentation significantly increased. The

main reason was an increase in the number of dislocations emanating from the grain boundary. The dislocation emission from the grain boundary restricted the penetration of the indenter and limited the formation of the octahedral slip systems of type {111}<110>, and consequently, the required force for indentation increased.

References

1. Salehinia, I., Wang, J., Bahr, D.F., Zbib, H.M.: Molecular dynamics simulations of plastic deformation in Nb/NbC multilayers. Int. J. Plast. **59**(0), 119–132 (2014). doi:10.1016/j.ijplas.2014.03.010
2. Matsumoto, R., Nakagaki, M., Nakatani, A., Kitagawa, H.: Molecular-dynamics study on crack growth behavior relevant to crystal nucleation in amorphous metal. CMES **9**, 75–84 (2005)
3. Yu, H.-L., Lu, C., Tieu, K., Deng, G.-Y.: A numerical model for simulation of crack initiation around inclusion under tensile load. J. Comput. Theor. Nanosci. **9**, 1745–1749 (2012)
4. Tomohito, T., Yoji, S.: Atomistic simulations of elastic deformation and dislocation nucleation in Al under indentation-induced stress distribution. Model. Simul. Mater. Sci. Eng. **14**(5), S55 (2006)
5. Verkhovtsev, A.V., Yakubovich, A.V., Sushko, G.B., Hanauske, M., Solov'yov, A.V.: Molecular dynamics simulations of the nanoindentation process of titanium crystal. Comput. Mater. Sci. **76**(0), 20–26 (2013). doi:10.1016/j.commatsci.2013.02.015
6. Huo, D., Liang, Y., Cheng, K.: An investigation of nanoindentation tests on the single crystal copper thin film via an atomic force microscope and molecular dynamics simulation. Proc. Inst. Mech. Eng. Part C J. Mech. Eng. Sci. **221**(2), 259–266 (2007). doi:10.1243/0954406jmes448
7. Nair, A.K., Parker, E., Gaudreau, P., Farkas, D., Kriz, R.D.: Size effects in indentation response of thin films at the nanoscale: a molecular dynamics study. Int. J. Plast. **24**(11), 2016–2031 (2008). doi:10.1016/j.ijplas.2008.01.007
8. Kim, K.J., Yoon, J.H., Cho, M.H., Jang, H.: Molecular dynamics simulation of dislocation behavior during nanoindentation on a bicrystal with a $\Sigma = 5$ (210) grain boundary. Mater. Lett. **60**(28), 3367–3372 (2006). doi:10.1016/j.matlet.2006.03.020
9. Fang, T.-H., Wu, J.-H.: Molecular dynamics simulations on nanoindentation mechanisms of multilayered films. Comput. Mater. Sci. **43**(4), 785–790 (2008). doi:10.1016/j.commatsci.2008.01.066
10. Liao, M.-L., Weng, M.-H., Ju, S.-P., Chiang, H.-J.: Molecular dynamics simulation on the nanoindentation behavior of a copper bilayered thin film. Chin. J. Catal. **29**(11), 1122–1126 (2008). doi:10.1016/S1872-2067(09)60012-7
11. Plimpton, S.: Fast parallel algorithms for short-range molecular dynamics. J. Comput. Phys. **117**, 1–19 (1995)
12. Stukowski, A.: Visualization and analysis of atomistic simulation data with OVITO—the Open Visualization Tool. Model. Simul. Mater. Sci. Eng. **18**, 015012 (2010). doi:10.1088/0965-0393/18/1/015012
13. Mishin, Y., Farkas, D., Mehl, M.J., Papaconstantopoulos, D.A.: Interatomic potentials for monoatomic metals from experimental data and ab initio calculations. Phys. Rev. B **59**(5), 3393 (1999)
14. Nejadseyfi, O., Shokuhfar, A.: Molecular dynamics simulation of the effects of crystal orientation and grain boundary misorientation angle on the nano-crack growth. J. Comput. Theor. Nanosci. **11**(10), 2199–2207 (2014)
15. Liu, T., Groh, S.: Atomistic modeling of the crack–void interaction in α-Fe. Mater. Sci. Eng. A **609**(0), 255–265 (2014). doi:10.1016/j.msea.2014.05.005
16. Yuan, Y., Sun, T., Zhang, J., Yan, Y.: Molecular dynamics study of void effect on nanoimprint of single crystal aluminum. Appl. Surf. Sci. **257**(16), 7140–7144 (2011). doi:10.1016/j.apsusc.2011.03.073
17. Meguid, S.A., Al Jahwari, F.: Modeling the pullout test of nanoreinforced metallic matrices using molecular dynamics. Acta Mech. **225**(4–5), 1267–1275 (2014). doi:10.1007/s00707-013-1065-1
18. Ju, S.P., Wang, C.T., Chien, C.H., Huang, J.C., Jian, S.R.: The nanoindentation responses of nickel surfaces with different crystal orientations. Mol. Simul. **33**(11), 905–917 (2007). doi:10.1080/08927020701392954
19. Li, D., Wang, F., Yang, Z., Zhao, Y.: How to identify dislocations in molecular dynamics simulations? Sci. China Phys. Mech. Astron. **57**(12), 2177–2187 (2014). doi:10.1007/s11433-014-5617-8
20. Muhammad, I., Fayyaz, H., Muhammad, R., Ahmad, S.A.: Dynamic characteristics of nanoindentation in Ni: a molecular dynamics simulation study. Chin. Phys. B **21**(11), 116201 (2012)
21. Liang, Y., Wang, Q., Yu, N., Chen, J., Zha, F., Sun, Y.: Study of dislocation nucleation mechanism in nanoindentation process. Nanosci. Nanotechnol. Lett. **5**(5), 536–541 (2013)
22. Kim, K.J., Yoon, J.H., Cho, M.H., Jang, H.: Molecular dynamics simulation of dislocation behavior during nanoindentation on a bicrystal with aΣ = 5 (210) grain boundary. Mater. Lett. **60**(28), 3367–3372 (2006)
23. Li, J., Soh, A.K.: Toughening of nanocrystalline materials through shear-coupled migration of grain boundaries. Scr. Mater. **69**(4), 283–286 (2013). doi:10.1016/j.scriptamat.2013.04.014
24. Farkas, D., Frøseth, A., Van Swygenhoven, H.: Grain boundary migration during room temperature deformation of nanocrystalline Ni. Scr. Mater. **55**(8), 695–698 (2006). doi:10.1016/j.scriptamat.2006.06.032
25. Wan, L., Wang, S.: Shear response of the Σ9<110>{221} symmetric tilt grain boundary in fcc metals studied by atomistic simulation methods. Phys. Rev. B Condens. Matter **82**(21), 214112 (2010)